

WAVELET BASED PALMPRINT RECOGNITION

XIANG-QIAN WU ^(a), KUAN-QUAN WANG ^(a), DAVID ZHANG ^(b)

^(a) Biometrics Research Center, Dept. of Computer Science and Engineering
Harbin Institute of Technology, Harbin 150001, P. R. China

^(b) Department of Computing, Hong Kong Polytechnic University, Hong Kong
E-MAIL: csxqw@yaho.com, wangkq@hope.hit.edu.cn, csdzhang@comp.polyu.edu.hk

Abstract:

Palmprint is a new biometric method to recognize a person. The features in a palmprint include principal lines, wrinkles and ridges, etc. Line structure feature, which includes principal lines and wrinkles, is one of the most popular methods in palmprint recognition. However, the line structure feature does not contain the thickness and width information of principal lines and wrinkles, which are very important to discriminate palmprints. Ridges are not included in line structure feature either. So these methods cannot distinguish different palmprints with similar line structure. Furthermore, the line extraction is a difficult task. The fact that principal lines, wrinkles and ridges have different resolutions motivates us to analyze the palmprint using multi-resolution analysis method. A novel palmprint feature, named wavelet energy features, is defined employing wavelet, which is a powerful tool of multi-resolution analysis, in this paper. WEF can reflect the wavelet energy distribution of the principal lines, wrinkles and ridges in several directions at different wavelet decomposition level (scale), so its ability to discriminate palms is very strong. Easiness to compute is another virtue of WEF. The very high recognition rates obtained in experiments shows the effect of the proposed method.

Keywords:

Biometrics; Palmprint recognition; Feature extraction; Wavelet energy feature

1 Introduction

Computer-aided personal recognition becomes more and more important in this information era. Biometrics is one of the most important and reliable methods in this field ^[1]. The most widely used biometric feature is the fingerprint ^[2] while the most reliable one is the iris ^[3]. Palmprint, as a new biometric feature, has several advantages compared with other ones: low-resolution imaging, low-cost capture device, non-fake, stable line feature and easy self-positioning, etc. It is for this reason that palmprint recognition draws more and more researchers' attention recently ^[4-5, 7-8].

There are many features in a palmprint ^[4] such as principal lines, wrinkles and ridges, etc. The popular feature used in palmprint recognition is the line structure feature including principal lines and wrinkles. Nevertheless, there are many problems in the line structure feature based

palmprint recognition system: firstly, the lines are very difficult to be extracted because some palmprints are very unclear (See Fig. 1); secondly, principal lines and wrinkles are not enough to discriminate palms since there are many palmprints with similar line features (See Fig. 2); thirdly, the thickness and width of the different lines, which are very important to distinguish palms, are not considered in these system. In order to resolve these problems, a novel palmprint feature containing the information of principal lines, wrinkles and ridges should be defined.

In palmprint, different feature has different resolution. The principal lines are the thickest, so they can be analyzed in low resolution. The wrinkles are thinner than the principal lines and can be analyzed in medium resolution. The ridges are the thinnest, thus they must be analyzed in high resolution. Therefore, multi-resolution methods should be used to analyze the palmprint. Directional property is another important character of these features. Wavelet ^[9-10, 12] is a powerful tool of multi-resolution analysis and two-dimensional wavelet transformation can decompose the image in several directions at different resolutions (scale). Hence, Wavelet has been used widely in biometrics based personal recognition systems ^[6, 11].

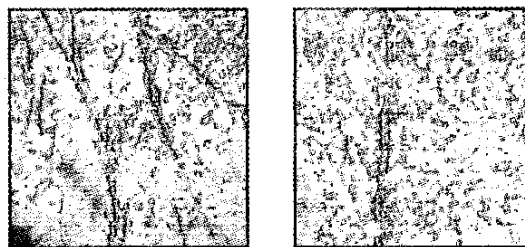


Fig.1. Some unclear lines palmprint images

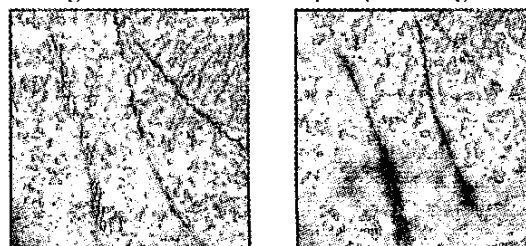


Fig.2. Some palmprints with similar lines

Moreover, to nonoscillating pattern, the amplitudes of wavelet coefficients increase when the scale of wavelet decomposition increase, however, to a high frequency oscillating pattern, the amplitudes of wavelet coefficients at large scales are much smaller than at fine scale which matches the spatial frequency of the oscillations [10]. In a palmprint, the principal lines and wrinkles are nonoscillating patterns while the ridges are oscillating pattern, so the distributions of their wavelet energy, which is defined using wavelet coefficients, are different at each scale of wavelet decomposition. Therefore, wavelet energy is very suitable to describe a palmprint. Wavelet energy feature (WEF) of a palmprint is defined in this paper.

Observing the palms carefully, we find that the most features of them are concentrated in a central rectangle part of the palm. So we cut the central sub-image to represent the whole one in this paper.

The paper is organized as follows: In Section 2, two-dimensional wavelet transform is reviewed briefly. Section 3 describes the wavelet feature construction in details. Experimental results are given in Section 4, and Section 5 gives a conclusion.

2 Two-dimensional Wavelet Transform (2D WT)

We call a function two-dimensional smoothing function if its double integral is nonzero. We define two wavelets [9] that are, respectively, the partial derivatives along x and y of a two-dimensional smoothing function $\theta(x, y)$:

$$\psi^1(x, y) = \frac{\partial \theta(x, y)}{\partial x} \quad (1)$$

$$\psi^2(x, y) = \frac{\partial \theta(x, y)}{\partial y} \quad (2)$$

Let $\psi_s^1(x, y) = (1/s)^2 \psi^1(x/s, y/s)$ and $\psi_s^2(x, y) = (1/s)^2 \psi^2(x/s, y/s)$. For any function $f(x, y) \in L^2(R^2)$, the wavelet transform defined with respect to $\psi_s^1(x, y)$ and $\psi_s^2(x, y)$ has two components [10]:

$$W^1 f(s, x, y) = f * \psi_s^1(x, y) \quad (3)$$

$$W^2 f(s, x, y) = f * \psi_s^2(x, y) \quad (4)$$

It is an efficient way to implement discrete wavelet transform (DWT) using filters [12], which was developed by Mallat in 1988. K^{th} -level wavelet decomposition is shown in Fig. 3, where A_{k-1} is the approximation coefficients of the $(K-1)^{\text{th}}$ -level decomposition, A_k, H_k, V_k and D_k are the approximation, horizontal, vertical and diagonal detail coefficients of the K^{th} -level decomposition, respectively. A_0 is the original image I . So after decomposed on J^{th} -level, the original image I is represented by $3J+1$ sub-images:

$$[A_J, (H_i, V_i, D_i)_{i=1, \dots, J}] \quad (5)$$

where A_J is a low resolution approximation of original image, and H_i, V_i, D_i are the wavelet sub-images containing the image details in horizontal, vertical and diagonal directions at different scales (2^i). The large amplitudes in $H_i, V_i, D_i (1 \leq i \leq J)$ correspond to the horizontal high frequency (horizontal edge), vertical high frequency (vertical edge) and diagonal high frequency (vertical diagonal), respectively. Fig. 4 shows an example of the 2-level DWT decomposition of an image.

3 Wavelet Feature Extraction

3.1 Wavelet Energy

The wavelet energy in horizontal, vertical and diagonal directions at i^{th} level can be, respectively, defined as:

$$E_i^h = \sum_{x=1}^M \sum_{y=1}^N (H_i(x, y))^2 \quad (6)$$

$$E_i^v = \sum_{x=1}^M \sum_{y=1}^N (V_i(x, y))^2 \quad (7)$$

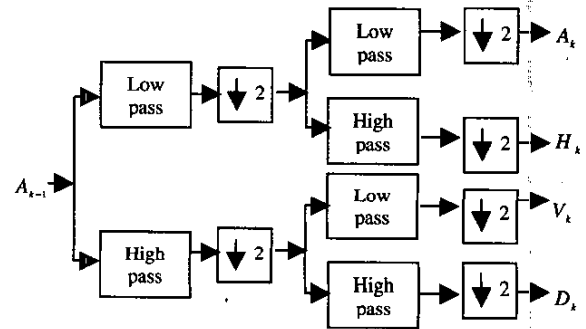
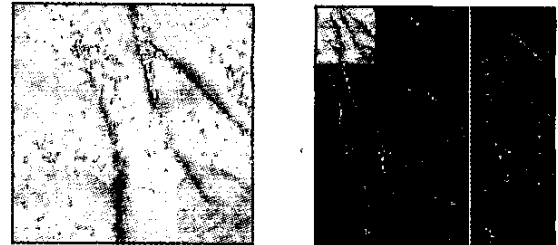


Fig.3. One-level DWT decomposition



(a) Original image

(b) 2-level wavelet decomposition

Fig.4. An example of wavelet decomposition

$$E_i^d = \sum_{x=1}^M \sum_{y=1}^N (D_i(x, y))^2 \quad (8)$$

These energies reflect the strength of the images' details in different direction at the i^{th} wavelet decompose level. The details of a palmprint are the principal lines, wrinkles and ridges, etc. Hence, Eq. (6) – (8) can describe the intensity of these features in different orientation at the i^{th} wavelet decomposition level (scale). In addition, because the amplitudes of wavelet coefficients of nonoscillating pattern increase with the extension of wavelet decomposition scale while that of a high frequency oscillating pattern at large scales are much smaller than at fine scale which matches the spatial frequency of the oscillations [10], the energy of principal lines and wrinkles, which are nonoscillating patterns, are concentrated at the large wavelet decomposition scales and the most energy of ridges, which are oscillating pattern, are focused at the small scales. So the feature vector,

$$(E_i^h, E_i^v, E_i^d)_{i=1,2,\dots,M}, \quad (9)$$

where M is the total wavelet decomposition level, can describe the global details feature of a palm effectively.

3.2 Wavelet Energy Feature (WEF) Construction

As we mentioned above, the vectors computed from Eq. (6) – (9) are global features of a palm. These features extracted from the whole images don't preserve the information concerning the spatial location of different details, so its ability to describe a palm is weak. In order to deal with this problem, we can divide the detail images into $S \times S$ non-overlap blocks equally (Fig. 5), and then compute the energy of each block. Thirdly, the energies of all blocks are used to construct a vector. Finally, the vector is normalized by the total energy. This normalized vector is named *wavelet energy feature (WEF)*. If an image is decomposed to J level, the length of its WEF is $3 \times S \times S \times J$.

WEF has a strong ability to distinguish palmprints as shown in Fig. 6 and 7. The images in these figures are decomposed to $M = 3$ level, and each wavelet details image is divided into 4×4 blocks. So the length of WEFs is 144. Fig. 8 shows the difference between the corresponding components of the WEFs in Fig. 6 and 7. According to these figures, WEFs of the palmprints from the same palm are very similar while those from different palms are quite dissimilar.

Note that there are three peaks in each palm's WEF. These peaks correspond to the energy of blocks traversed by principal lines in the vertical detail image at each scale. The energy of the principal lines is prominent in a palm and the principal lines' directions are almost vertical in these figures, so the energy of these blocks in the vertical detail images are larger than those of the blocks not containing the principal lines and the corresponding ones in other detail images. Therefore, there exists a peak in

corresponding position at each decomposition scale in WEF. The position of the principal lines of Fig. 7 (a), (b) are similar, so the peaks of their WEFs occur at almost same position (see Fig. 7 (c)).

3.3 WEF based Palmprint Recognition

WEF of a palmprint is computed as below:

- 1) Orientate the palmprint image.
- 2) Crop a $N \times N$ rectangular sub-image from the center of the palm.
- 3) Decompose this sub-image to J scale by wavelet transform.
- 4) Divide each detail image into $S \times S$ non-overlapping blocks.
- 5) Compute the energy of each block and construct a $3 \times S \times S \times J$ dimensional vector.
- 6) Normalize this vector by the total energy and form the WEF.

Palmprint recognition includes two stages: training stage and recognition stage.

In the training stage, WEFs of the training samples are computed, and the template of a palm is obtained by averaging the WEFs of all training samples captured from the same palm.

In the recognition stage, WEF of the input palm is computed firstly; and then compared with all the registered templates; finally, find the most similar template and take it as the recognition result.

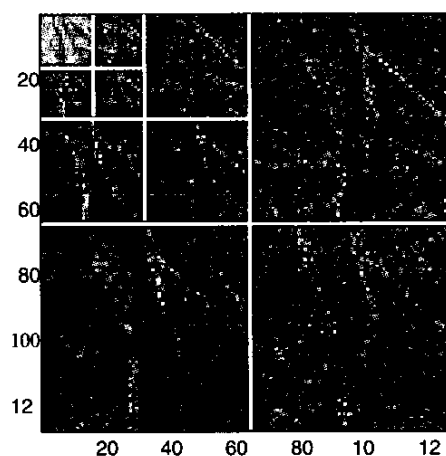


Fig.5. The division of the detail images at each scale

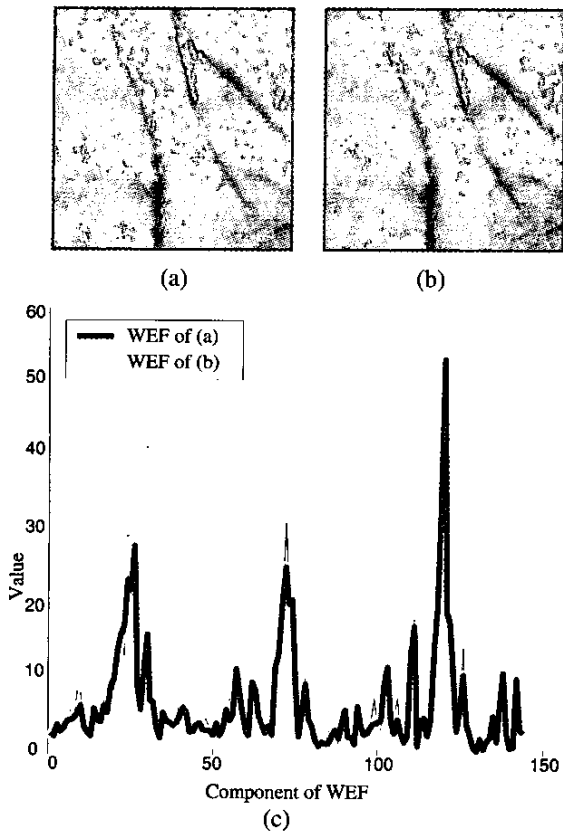


Fig.6. Palmprints captured from the same palm and their corresponding WEF

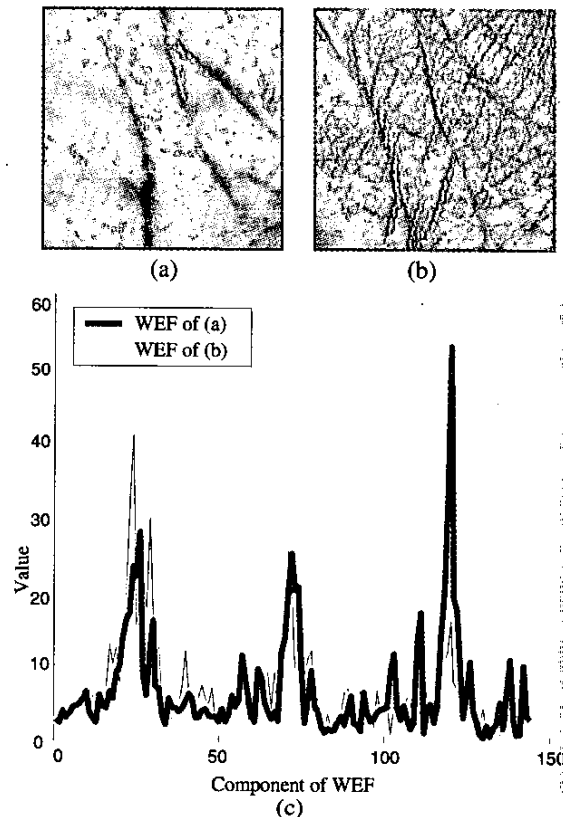


Fig.7. Palmprints captured from different palms and their corresponding WEF

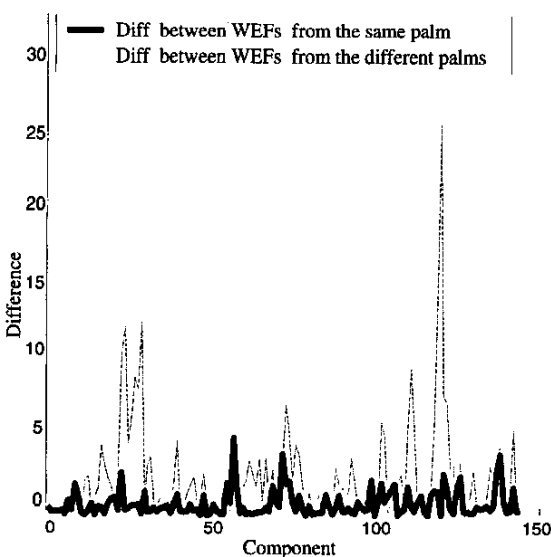


Fig.8. The difference of WEFs in Figure 6 and 7

4 Experimental Results

A database of 1,000 palmprint images from 200 palms are used for experiments. These palmprints are taken from different age, sex people by the same device in Hongkong Polytechnic University. 5 images are captured from each palm in which four are used to train template and the remaining one is the testing sample. The resolution of these images is 320×240 with 256 grayscales. The 128×128 central part of each palmprint is cropped to represent the whole one. Each detail image is divided into 4×4 non-overlapping blocks. The cityblock distance is used to describe the similarity between WEFs. All the experiments are conducted with Matlab 6.1 on PIII 1G, 256M RAM PC.

We have tested our method using different wavelets and different wavelet decomposition levels. The wavelets chosen here are those used for fingerprint recognition in [6]. The recognition rates are listed in Tab. 1. The first row is the levels the image is decomposed to and the first column are

the wavelet name in which 'Db' and 'Sym' are the abbreviation for Daubechies wavelet and Symmlet orthonormal wavelet, respectively, and the numbers is the vanishing moments of the corresponding wavelet filters.

According to Tab. 1, the highest recognition rate, 99.5%, is obtained at the 4 level decomposition when the wavelet is chosen as Symmlet and the vanishing moment is 4. Also, 99.0% recognition rates are gotten when using Harr wavelet (3 level), Daubechies wavelet with 9 and 10 vanishing moments (4 level) and Symmlet wavelet with 9 vanishing moment (4 - 6 level). Considering other factors such as storage and computation complex, etc., Harr wavelet, the simplest wavelet, is the best choice to palmprint recognition for our database when the images are decomposed to 3 scales.

The total training time using Harr wavelet at 3 levels is 187 seconds and the average testing time is 0.29 second (not include the orientation time). It is enough for an online palmprint recognition system.

5 Conclusion

According to the fact that the different features have different resolution on palm, a novel palmprint feature, named wavelet energy feature (WEF), is defined based on wavelet in this paper. WEF can reflect the wavelet energy distribution of the principal lines, wrinkles and ridges at different scales, so it can discriminate palmprints effectively. The experimental results show that Harr wavelet decomposition to 3 scales is the most suitable for online palmprint recognition.

Acknowledgements

Supported by the National High Technology Research and Development Program of China (863-306-ZD13-06-1)

References

[1] D. Zhang, *Automated Biometrics - Technologies and Systems*, Kluwer Academic Publishers, 2000.
 [2] Jain, L. Hong and R. Bolle, "On-line fingerprint verification," *IEEE Trans. Pattern Analysis and Machine Intelligence*, vol. 19, no. 4, pp. 302-313, 1997.
 [3] Daugman, J., "High confidence recognition of persons by iris patterns," *IEEE 35th International Carnahan Conference on Security Technology*, pp. 254 -263, 2001.
 [4] Dapeng Zhang, Wei Shu, "Two novel characteristics in palmprint verification: datum point invariance and line feature matching," *Pattern Recognition*, vol. 32, pp. 691-702, 1999.
 [5] Shu Wei, Zhang D, "Automated personal identification by palmprint," *Optical Engineering*, vol. 37, no. 8, pp. 2359-2362, 1998.

[6] Tico, M.; Immonen, E.; Ramo, P.; Kuosmanen, P.; Saarinen, J, "Fingerprint recognition using wavelet features," *The 2001 IEEE International Symposium on Circuits and Systems*, vol. 2. Pp. 21 -24, 2001.
 [7] Shu Wei, Zhang D, "Biometric identification by palmprint," In *Proceedings of CISS'98*, Princeton, New Jersey, USA, pp. 254-258, 1998.
 [8] Shu Wei, Zhang D, "Palmprint Verification: An implementation of Biometric Technology," In *Proceedings of ICPR'98*, Brisbane, Queensland, Australia, pp. 219-221, 1998.
 [9] Mallat, S. and Zhong, S, "Characterization of signals from multiscale edges," *IEEE Trans. Pattern Analysis and Machine Intelligence*, vol. 14, no. 7. Pp. 710- 732, 1992.
 [10] Mallat, S.; Hwang, W.L, "Singularity detection and processing with wavelets," *IEEE Trans. Information Theory*, vol. 38, no. 2. Pp. 617- 643, 1992.
 [11] Boles, W.W.; Boashash, B, "A human identification technique using images of the iris and wavelet transform", *IEEE Trans. Signal Processing*, vol. 46. pp. 1185-1188, 1998.
 [12] Rioul, O.; Vetterli, M, "Wavelets and signal processing," *IEEE Signal Processing Magazine*, vol. 8, no. 4, pp. 14-38, 1991.

Table. 1 Recognition Rates (%)

Scale wavelet	1	2	3	4	5	6
Harr	91.5	97.0	99.0	98.5	98.0	98.0
Db 2	89.5	94.0	95.0	98.0	97.5	97.5
Db 3	90.0	94.0	96.5	98.0	97.0	97.0
Db4	88.0	95.5	97.0	98.5	98.5	98.5
Db 5	89.5	95.0	95.5	98.5	97.5	97.5
Db 6	89.0	95.5	97.5	98.0	98.5	98.5
Db 7	87.0	95.5	97.5	97.5	98.0	98.0
Db 8	89.0	95.0	98.0	98.5	98.0	98.0
Db 9	88.0	95.0	98.0	99.0	98.5	98.5
Db10	87.5	96.0	98.0	99.0	97.5	97.5
Sym4	88.5	94.0	97.0	97.5	97.5	97.5
Sym5	88.0	96.0	97.5	99.5	98.5	98.5
Sym6	88.5	94.0	97.0	97.5	97.5	97.5
Sym7	88.0	93.5	97.5	98.5	98.0	98.0
Sym8	88.5	94.5	97.5	98.5	97.5	97.5
Sym9	88.5	96.5	97.5	99.0	99.0	99.0
Sym10	88.5	95.0	97.5	98.0	98.0	98.0